# ANALYSIS OF OCEAN WAVE BY AIRBORNE PI-SAR X-BAND IMAGES

Chan-Su Yang*, Kazuo Ouchi**

* Korea Ocean Satellite Center
Ocean Satellite Remote Sensing & Observation Technology Research Department
Korea Ocean Research & Development Institute
1270 Sa-2-dong Sangrok-gu Ansan-city, 426-744, Korea
E-mail: yangcs@kordi.re.kr
**Department of Computer Science
National Defence Academy
1-10-20 Hashirimizu, Yokosuka, Kanagawa, 239-8686 Japan

ABSTRACT In the present article, we analyze airborne Pi-SAR (Polarimetric-Interferometric SAR) X-band images of ocean waves around the Miyake Island at approximately 180 km south from Tokyo, Japan. Two images of a same scene were produced at approximately 40 min. interval from two directions at right angles. One image shows dominant range travelling waves, but the other image shows a different wave pattern. This difference can be caused by the different image modulations of RCS and velocity bunching. We have estimated the dominant wavelength from the image of range waves, and from the wave phase velocity computed from the dispersion relation (though no wave height data were available), the image intensity is computed by using the velocity bunching model. The comparison of the result with the second image at right angle strongly suggests the evidence of velocity bunching.

**KEY WORDS:** Ocean Wave, Airborne Pi-SAR, Velocity Bunching

## 1. INTRODUCTION

Analysis of ocean waves using synthetic aperture radar (SAR) images is an important issue in oceanography, not only for an academic interest but also for validation and improvement of wave forecasting models and for the utilization in shipping industry and in the field of maritime disaster prevention. Since the launch of the SEASAT satellite with a L-band SAR in 1978, considerable effort has been made to understand the SAR imaging mechanisms of ocean waves, and a large number of publications are available. Consequently, the principal mechanisms of imaging ocean waves by SAR are considered to be well understood.

According to the present knowledge, there appear 4 major image modulations to contribute to SAR image formation of ocean waves (Hasselmann et al., 1985). The first is the RCS (Radar Cross Section) modulation which is largest for range travelling waves and vanishes for azimuth travelling waves. The second is the velocity bunching modulation arising from the wave motion. This modulation is inherent to SAR, and it is largest for azimuth waves and vanishes for range waves. The third and fourth are the tilt and hydrodynamic modulations associated with the small-scale waves. Among these modulations, velocity bunching still requires some attention, because its theory is not yet, in a strict sense, confirmed by experiment.

In the present article, we analyse airborne Pi-SAR (Polarimetric-Interferometric SAR) X-band images of ocean waves around the Miyake Island at approximately 180 km south from Tokyo, Japan. Two images of a same scene were produced at approximately 40 min. interval from two directions at right angles. One image shows dominant range travelling waves, but the other image shows a different wave pattern. This difference can be caused by the different image modulations of RCS and velocity bunching. We have estimated the dominant wavelength from the image of range waves, and from the wave phase velocity computed from the dispersion relation (though no wave height data were available), the image intensity is computed by using the velocity bunching model (Ouchi & Burridge, 1994).

## 2. PI-SAR SYSTEM

Since 1995, National Institute of Information and Communications Technology (NICT) and Japan

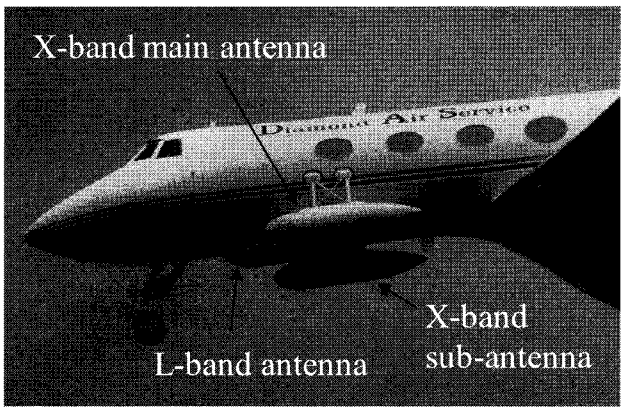


Figure 1. Installed Pi-SAR system.

Aerospace Exploration Agency (JAXA) have collaborated to develop an airborne high-resolution multiparameter synthetic aperture radar. This synthetic aperture radar is a dual frequency radar operating at L-band and X-band frequencies with polarimetric functions. The X-band system also has an interferometric function by which topographic mapping of the ground surface is achieved. The development of the L-band and the X-band parts was carried out by JAXA and NICT, respectively.

Pi-SAR observes the ground surface using dual frequencies simultaneously with the X-band ($\lambda$ =3.14 cm) and the L-band ($\lambda$ =23.6 cm). The horizontal resolution is 1.5 m for the X-band and 3 m for the L-band, and it is capable of polarimetric observation (by transmitting/receiving horizontal and vertical polarized waves). Pi-SAR also had features for an interferometric function to provide elevation profiles of the ground using two antennas through X-band observations. Table 1 shows the major specifications of Pi-SAR.

For the polarimetric function, the X-band main-antenna is equipped to deal with both vertical and horizontal polarized waves. The sub-antenna, which is required for interferometry, employs vertically polarized waves, since the return power of these waves is relatively large. The two antennas should be firmly installed as far as possible because the fluctuations in the antenna's position, caused by airplane vibration, result in measurement errors. They are installed as shown in Figure 1, and antenna separation is 2.3 m in the Pi-SAR configuration. The roll angle is variable between 40 and 65 degree (peak to peak) to extend the range of incidence angle selectively for all target objects and observation modes. The dual-axis variable angle (within ±6.5 degree) mechanism control the yaw angle so that the antenna are kept parallel along the flight direction, regardless of the drift angle of the airplane.

Table 1 Specifications of NICT/JAXA Airborne SAR

| Frequency | X-band (9.55468913 GHz) | L-band (1.271490 GHz) |
|---|---|---|
| Range resolution | 1.5 m/3 m | 3 m/5 m /10 m/20 m (Variable) |
| Azimuth resolution | 1.5 m (4-look Processing) | 3 m (4-look Processing) |
| Noise equivalent NRCS | less than -40 dB | less than -40 dB |
| SNR | larger than 10 dB | larger than 10 dB |
| Interferometry Baseline Length /Topographic Height Resolution/Phase Accuracy | 2.3 m / 2 m / less than 5 deg. | N/A |
| Polarimetry Phase Accuracy | HH/HV/VV/VHless than 5 deg. | HH/HV/VV/VHless than 5 deg. |
| Incidence Angle | variable (10 -- 75 deg.) | variable (20 -- 60 deg.) |
| NRCS Measurement Accuracy | less than 0.5 dB | less than 0.5dB |
| Antenna Size | 105 cm(L) x 19 cm (W) | 155 cm (L) x 65 cm (W) |
| Antenna Type | Slotted Waveguide Array | Microstrip Patch Array |
| Transmit Power(HPA Peak Output) | 8.3 kW | 3.5 kW |
| Pulse Length | 10 microsec. | 10 microsec. |
| Transmitter Bandwidth | 100 MHz | 50 MHz |
| Transmitting/Receiving | all digital | all digital |
| Data Sampling Rate | 123.45/61.725 MHz | 61.7/30.9 |
| Data Quantization | 8 bits (I and Q) | 8 bits (I and Q) |
| Data Transfer Rate | 512 Mbps | 256 Mbps |
| Data Recorder | SONY/DIR1000 x 2 | SONY/DIR1000 x 1 |
| Developed by | NICT | JAXA |
| Manufacturer | NEC Corporation | NEC Corporation |

Here, the SSC (single-look, slant range, complex) data are used.

## 3. STUDY AREA AND METHOD

During the data acquisition on Feburuary 28, 2004, the Pi-SAR made a flight above Miyake-Oshima, Japan along a flight paths at right angle as shown in Figs. 2 and 3.

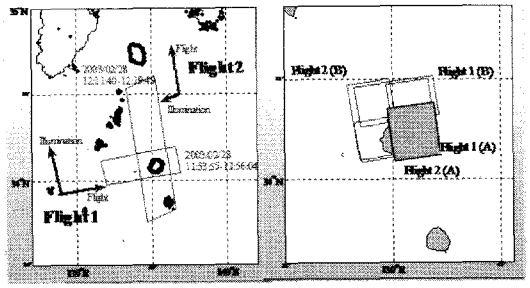


Figure 2. Flight paths (left image) and research area (right) in and around Miyake-Oshima, Japan on Feburuary 28, 2004(left).

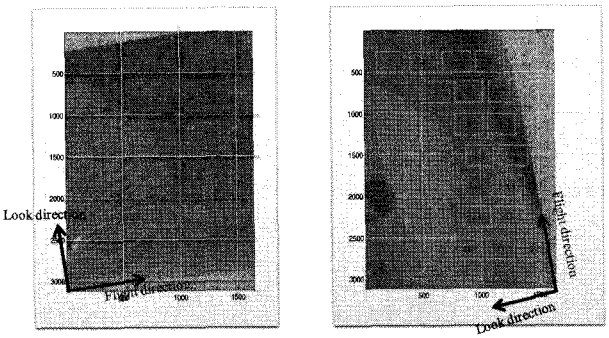


Figure 3. Geo-registered images. Flight 1 (left) and flight 2 (right). Red squares in right panel indicate sub-areas for wave spectrum analysis.

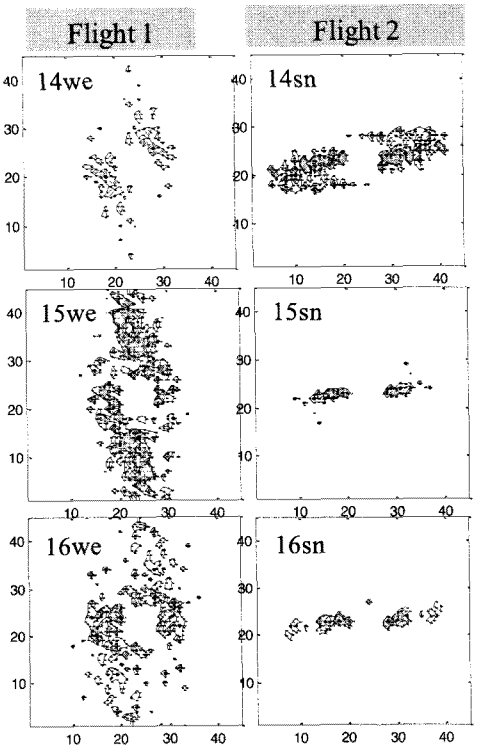


Figure 4. SAR image spectra.

18 subimages are extracted, and the directional wave spectra are compared to each other of the two different areas.

One image shows dominant range travelling waves, but the other image shows a different wave pattern. This difference can be caused by the different image modulations of RCS and velocity bunching.

We have estimated the dominant wavelength from the image of range waves, and from the wave phase velocity computed from the dispersion relation (though no wave height data were available), the image intensity is computed by using the velocity bunching model.

## 4. RESULTS

Wave imaging mechanisms were investigated using airborne Pi-SAR (Polarimetric-Interferometric SAR) X-band VV images of ocean waves. The comparison of the result with the second image at right angle strongly suggests the evidence of velocity bunching. Waves caused by velocity bunching are investigate and compared with the theory, and an estimated wave height was 2.5 m

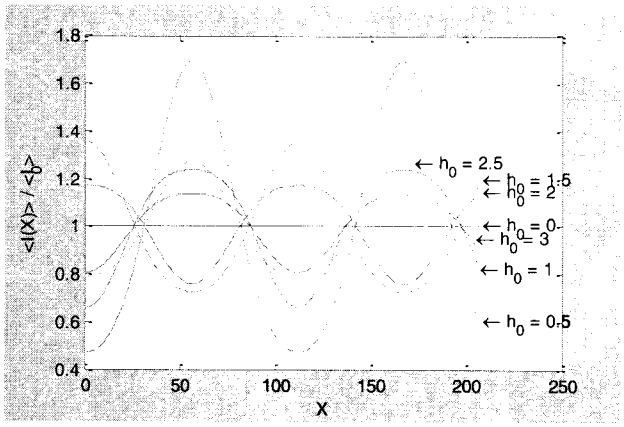


Figure 5. Theoretical Results <I>/<I_0>.


## ACKNOWLEDGEMENTS

This work was supported by the Basic Research Project, "Development of Management and Restoration Technologies for Estuaries" of KORDI and the Public Benefit Project of Remote Sensing, "Satellite Remote Sensing for Marine Environment" of Korea Aerospace Research Institute.


## REFERENCES


Hasselmann, K., R. K. Raney, W. J. Plant, W. Alpers, R. A. Shuchman, D. R. Lyzenga, C. L.Rufenach, and M. J. Tucker, 1985. Theory of synthetic aperture radar ocean imaging: a MARSEN view, *J. Geophy. Res.*, Vol. 90, No. C3, 4659-4686.

Ouchi, K. and D. A. Burridge, 1994. Resolution of a controversy surrounding the focusing mechanisms of synthetic aperture radar images of ocean waves," *IEEE Trans. Geosci. Remote Sens.*,Vol. 32, 1004-1016.